

## Caspase Activation by Anticancer Drugs: The Caspase Storm

Zhimin Tao,<sup>†</sup> Jerry Goodisman,<sup>\*,†</sup> Harvey S. Penefsky,<sup>‡</sup> and A.-K. Souid<sup>\*,§</sup>

Department of Chemistry, Syracuse University, 1-014 CST, Syracuse, New York 13244, Public Health Research Institute, 225 Warren Street, Newark, New Jersey 07103-3506, and Department of Pediatrics, State University of New York, Upstate Medical University, 750 East Adams Street, Syracuse, New York 13210

Received January 2, 2007; Revised Manuscript Received March 12, 2007; Accepted March 16, 2007

**Abstract:** This study measures the time-dependence of cellular caspase activation by anticancer drugs and compares it with that of cellular respiration. Intracellular caspase activation and cellular respiration were measured during continuous exposure of Jurkat, HL-60, and HL-60/MX2 (deficient in topoisomerase-II) cells to dactinomycin, doxorubicin, and the platinum (Pt) compounds cisplatin, carboplatin, and oxaliplatin. Caspase activation was measured using the fluorogenic compound *N*-acetyl-asp-glu-val-asp-7-amino-4-trifluoromethyl coumarin (Ac-DEVD-AFC). We show that this substrate rapidly enters cells where it is efficiently cleaved at the aspartate residue by specific caspases, yielding the fluorescent compound 7-amino-4-trifluoromethyl coumarin (AFC). Following cell disruption, released AFC was separated on HPLC and detected by fluorescence. The appearance of AFC in cells was blocked by the pancaspase inhibitor benzylloxycarbonyl-val-ala-asp-fluoromethylketone, thus establishing that intracellular caspases were responsible for the cleavage. Caspase activity was first noted after about 2 h of incubation with doxorubicin or dactinomycin, the production of AFC being linear with time afterward. Caspase activation by doxorubicin was delayed in HL-60/MX2 cells, reflecting the critical role of topoisomerase-II in doxorubicin cytotoxicity. For both drugs, caspase activity increased rapidly between ~2 and ~6 h, went through a maximum, and decreased after ~8 h ("caspase storm"). Cisplatin treatment induced noticeable caspase activity only after ~14 h of incubation, and the fluorescent intensity of AFC became linear with time at ~16 h. Exposure of the cells to all of the drugs studied led to impaired cellular respiration and decreased cellular ATP, concomitant with caspase activation. Thus, the mitochondria are rapidly targeted by active caspases.

**Keywords:** Apoptosis; caspase; cisplatin; carboplatin; dactinomycin; doxorubicin; fluorogenic

### Introduction

Apoptosis is the principal mechanism of tumor cell death by chemotherapy.<sup>1</sup> This intracellular process is mediated, at

least partially, by a series of cysteine (aspartate-directed) proteases, termed *caspases*.<sup>2</sup> These proteases are synthesized as inactive precursors which are activated sequentially in a cascade that executes apoptosis.<sup>3</sup> The cellular inhibitory apoptosis proteins (cIAPs) bind to and inhibit active caspases.<sup>4</sup>

\* To whom correspondence should be addressed. J.G.: Department of Chemistry, Syracuse University, 1-014 CST, Syracuse, NY 13244; tel, 315-443-3035; fax, 315-443-4070; e-mail, goodisma@mailbox.syr.edu. A.-K.S.: tel, 315-464-5294; fax, 315-464-7238; e-mail, souida@upstate.edu.

<sup>†</sup> Syracuse University.

<sup>‡</sup> Public Health Research Institute.

<sup>§</sup> Upstate Medical University.

(1) Hengartner, M. O. The biochemistry of apoptosis. *Nature* **2000**, 407, 770–776.

(2) Earnshaw, W. C.; Martins, L. M.; Kaufmann, S. H. Mammalian caspases: structure, activation, substrate, and functions during apoptosis. *Annu. Rev. Biochem.* **1999**, 68, 383–424.

Apoptosis is initiated by activating specific cell surface receptors (e.g., tumor necrosis factor receptor and CD95, or Fas/APO-1) or intracellular targets (e.g., the pro-apoptotic Bcl-2 family member Bid). The resulting signals permeabilize the outer mitochondrial membrane, resulting in release of soluble proteins (e.g., cytochrome *c* and SMAC/Diablo) from the mitochondrial intermembrane space.<sup>5</sup> In the presence of ATP, released cytochrome *c* binds to Apaf-1 (apoptotic protease-activating factor 1), forming an oligomer (apoptosome) that activates caspases. Cytochrome *c*- and apoptosome-independent pathways for caspase activation are also known.<sup>6</sup> If caspases are blocked by zVAD-fmk,<sup>7</sup> the mitochondrial electrochemical potential ( $\Delta\psi$ ) can be regenerated despite cytochrome *c* leakage.<sup>8</sup>

Doxorubicin, an anthracycline antibiotic, is a widely used anticancer drug.<sup>9</sup> It intercalates with DNA and produces DNA breaks by stimulating topoisomerase-II cleavable complex formation.<sup>10</sup> In the cell, the quinone moiety of doxorubicin is reduced to the semiquinone radical, generating reactive oxygen species, which directly damage cell organelles. Oxidative damage produced by the drug is partially mediated by the doxorubicin–Fe(III) complex.<sup>11</sup> The outcome of these events is cell death, primarily by apoptosis.<sup>12</sup> Clinically, the maximum concentration of plasma doxorubicin after 30–60 mg/m<sup>2</sup> iv bolus dosing is 3–10  $\mu$ M, with half-lives<sup>13</sup> of  $t_{1/2\alpha} = 5.0 \pm 2.5$  min,  $t_{1/2\beta} = 1.9 \pm 0.6$  h, and  $t_{1/2\gamma} = 39 \pm 19$  h. However, cellular doxorubicin levels are

usually 30- to 100-fold higher than those of the plasma.<sup>13</sup> The *in vitro* studies presented here used somewhat higher concentrations for experimental convenience.

Dactinomycin is an important anticancer chromopeptide, commonly used *in vitro* to execute apoptosis. This drug intercalates between DNA base pairs and inhibits transcription.<sup>14</sup> The genomic injury leads to cell death, primarily by apoptosis. Clinically, the maximum concentrations of plasma dactinomycin after 0.7–1.5 mg/m<sup>2</sup> iv bolus dosing range<sup>15</sup> between 3 and 83 nM. Both dactinomycin and doxorubicin impair mitochondrial function during drug-induced apoptosis.<sup>16,17</sup> The effects of doxorubicin are less pronounced in cells deficient in topoisomerase-II (e.g., HL-60/MX2).<sup>18</sup> The *in vitro* studies presented here also employed higher drug concentrations.

The Pt-based compounds (cisplatin, carboplatin, and oxaliplatin) exert their antitumor activity by binding to DNA and promoting apoptosis.<sup>19–23</sup> Cisplatin, *cis*-diamminedichloroplatinum(II), is administered iv at  $\sim$ 20–120 mg/m<sup>2</sup> over 30–60 min, producing maximum plasma concentrations<sup>24</sup> of 5–25  $\mu$ M and  $t_{1/2}$  of  $\sim$ 30 min. In solutions with high chloride concentrations (e.g., human plasma), cisplatin exists

---

(3) Boatright, K. M.; Salvesen, G. S. Mechanism of caspase activation. *Curr. Opin. Cell Biol.* **2003**, *15*, 725–731.

(4) Shiozaki, E. N.; Chai, J.; Rigotti, D. J.; Riedl, S. J.; Li, P.; Srinivasula, S. M.; Alnemri, E. S.; Fairman, R.; Shi, Y. Mechanism of XIAP-mediated inhibition of caspase-9. *Mol. Cell* **2003**, *11*, 519–27.

(5) Green, D. R.; Kroemer, G. The pathophysiology of mitochondrial cell death. *Science* **2004**, *305*, 626–629.

(6) Hao, Z.; Duncan, G. S.; Chang, C-C; Elia, A.; Fang, M.; Wakeham, A.; et al. Specific ablation of the apoptotic functions of cytochrome *c* reveals a differential requirement of cytochrome *c* and Apaf-1 in apoptosis. *Cell* **2005**, *121*, 579–591.

(7) Sree, E. A.; Zhu, H.; Chow, S. C.; MacFarlane, M.; Nicholson, D. W.; Cohen, G. M. Benzylloxycarbonyl-Val-Ala-Asp (Ome) fluoromethylketone (Z-VAD-FMK) inhibits apoptosis by blocking the processing of CPP32. *Biochem. J.* **1996**, *315*, 21–24.

(8) Waterhouse, N. J.; Sedelies, K. A.; Sutton, V. R.; Pinkoski, M. J.; Thia, K. Y.; Johnstone, R.; et al. Functional dissociation of  $\Delta\psi$  and cytochrome *c* release defines the contribution of mitochondria upstream of caspase activation during granzyme B-induced apoptosis. *Cell Death Differ.* **2006**, *13*, 607–618.

(9) Binaschi, M.; Bigioni, M.; Cipollone, A.; Rossi, C.; Goso, C.; Maggi, C. A.; et al. Anthracyclines: Selected new developments. *Curr. Med. Chem.* **2001**, *1*, 113–130.

(10) Zunino, F.; Capranico, G. DNA topoisomerase II as the primary target of anti-tumor anthracyclines. *Anticancer Drug Des.* **1990**, *5*, 307–317.

(11) Kostoryz, E. L.; Yourtee, D. M. Oxidative mutagenesis of doxorubicin-Fe(III) complex. *Mutat. Res.* **2001**, *490*, 131–139.

(12) Bellarosa, D.; Ciucci, A.; Bullo, A.; Nardelli, F.; Manzini, S.; Maggi, C. A.; et al. Apoptotic events in a human ovarian cancer cell line exposed to anthracyclines. *J. Pharmacol. Exp. Ther.* **2001**, *296*, 276–283.

(13) Speth, P. A.; Linsen, P. C.; Boezeman, J. B.; Wessels, H. M.; Haanen, C. Cellular and plasma adriamycin concentrations in long-term infusion therapy of leukemia patients. *Cancer Chemother. Pharmacol.* **1987**, *20*, 305–310.

(14) Muller, W.; Crother, D. M. Studies of the binding of actinomycin and related compounds to DNA. *J. Mol. Biol.* **1968**, *35*, 251–290.

(15) Veal, G. J.; Cole, M.; Errington, J.; Parry, A.; Hale, J.; Pearson, A. D. J.; et al. Pharmacokinetics of dactinomycin in a pediatric patient population: a United Kingdom Children's Cancer Study Group study. *Clin. Cancer Res.* **2005**, *11*, 5893–5899.

(16) Tao, Z.; Withers, H. G.; Penefsky, H. S.; Goodisman, J.; Souid, A.-K. Inhibition of cellular respiration by doxorubicin. *Chem. Res. Toxicol.* **2006**, *19*, 1051–1058.

(17) Tao, Z.; Ahmad, S. S.; Penefsky, H. S.; Goodisman, J.; Souid, A.-K. Dactinomycin Impairs Cellular Respiration and Reduces Accompanying ATP Formation. *Mol. Pharmacol.* **2006**, *3*, 762–772.

(18) Harker, W. G.; Slade, D. L.; Drake, F. H.; Parr, R. L. Mitoxantrone resistance in HL-60 leukemia cells: Reduced nuclear topoisomerase II catalytic activity and drug-induced DNA cleavage in association with reduced expression of the topoisomerase II b isoform. *Biochemistry* **1991**, *30*, 9953–9961.

(19) Dabrowiak, J. C.; Goodisman, J.; Souid, A.-K. Kinetic study of the reaction of cisplatin with thiols. *Drug Metab. Dispos.* **2002**, *30*, 1378–1384.

(20) Hagrman, D.; Goodisman, J.; Dabrowiak, J. C.; Souid, A.-K. Kinetic study on the reaction of cisplatin with metallothionein. *Drug Metab. Dispos.* **2003**, *31*, 916–923.

(21) Hagrman, D.; Goodisman, J.; Souid, A.-K. Kinetic study on the reaction of platinum drugs with glutathione. *J. Pharmacol. Exp. Ther.* **2004**, *308*, 658–666.

(22) Tacka, K. A.; Szalda, D.; Souid, A.-K.; Goodisman, J.; Dabrowiak, J. C. Experimental and theoretical studies on the pharmacodynamics of cisplatin in Jurkat cells. *Chem. Res. Toxicol.* **2004**, *17*, 1434–1444.

(23) Goodisman, J.; Hagrman, D.; Tacka, K. A.; Souid, A.-K. Analysis of cytotoxicities of platinum compounds. *Cancer Chemother. Pharmacol.* **2006**, *57*, 257–267.

mostly in the dichloro neutral form, *cis*-Pt(NH<sub>3</sub>)<sub>2</sub>Cl<sub>2</sub>. However, at lower chloride concentrations, the drug takes on water, producing the charged species, *cis*-[Pt(NH<sub>3</sub>)(H<sub>2</sub>O)Cl]<sup>+</sup> and *cis*-[Pt(NH<sub>3</sub>)<sub>2</sub>(H<sub>2</sub>O)<sub>2</sub>]<sup>+2</sup>, and their deprotonation products, *cis*-[Pt(NH<sub>3</sub>)(OH)Cl], *cis*-[Pt(NH<sub>3</sub>)<sub>2</sub>(OH)(H<sub>2</sub>O)]<sup>+1</sup>, and *cis*-[Pt(NH<sub>3</sub>)<sub>2</sub>(OH)<sub>2</sub>]. In the presence of carbonate, carbonato and bicarbonato species are formed.<sup>25,26</sup> Within the nucleus, all these species may interact with nitrogen atoms on the bases of DNA, forming uni- and bidentate adducts. The resulting "Pt lesions" impair DNA function and promote cell death through apoptotic pathways.<sup>22,27</sup>

Carboplatin, *cis*-diammine(1,1-cyclobutanedicarboxylato)-platinum(II), and oxaliplatin, *trans*-1-diaminocyclohexane oxalatoplatinum, differ from cisplatin in that different types of ligands occupy the Pt coordination spheres. These newer Pt drugs exhibit unique antitumor activity and toxicity profiles. It is expected that the reactivity with DNA and induction of apoptosis by these compounds will differ from those of cisplatin.<sup>23</sup>

We recently described the effects of the above anticancer drugs on cellular respiration and on the accompanying ATP formation in Jurkat, HL-60, and HL-60/MX2 cells.<sup>16,17,22,23,27</sup> Doxorubicin-treated Jurkat and HL-60 cells exhibited almost constant rates of cellular respiration during the first 150 min of incubation; these rates were approximately equal to the rates for untreated cells. Thereafter, respiratory rates of treated cells decreased, to remain constant at a lower level. Respiration in HL-60/MX2 cells,<sup>18</sup> on the other hand, was less sensitive to doxorubicin.<sup>16</sup> In the presence of dactinomycin, the rate of respiration in the three cell lines studied decreased gradually with time.<sup>17</sup> With either drug, the inhibition of respiration was completely blocked by the pancaspase inhibitor zVAD-fmk.<sup>16,17</sup>

This study reports measurements of intracellular caspase activation during continuous exposure of cells to doxorubicin, dactinomycin, or Pt drugs. The purpose of the experiments was to compare the time-dependence of intracellular caspase activation with the time-dependences of inhibition of cellular respiration and ATP formation, and to determine if these profiles differed for different cells or different drugs. We used the fluorogenic compound Ac-DEVD-AFC which, as we show here, is rapidly absorbed by the cells in this study

(24) Soid, A.-K.; Dubowy, R. L.; Blaney, S.; Hershon, L.; Sullivan, J.; McLeod, W.; et al. Phase I clinical and pharmacologic study of weekly cisplatin and irinotecan combined with amifostine for refractory solid tumors (Children Oncology Group trial 9970). *Clin. Cancer Res.* **2003**, *9*, 703–710.

(25) Centerwall, C. R.; Goodisman, J.; Kerwood, D. J.; Dabrowiak, J. C. Cisplatin carbonato complexes: Implications for uptake, antitumor effects, and cytotoxicity. *J. Am. Chem. Soc.* **2005**, *127*, 12768–12769.

(26) Di Pasqua, A. J.; Goodisman, J.; Kerwood, D. J.; Toms, B. B.; Dubowy, R. L.; Dabrowiak, J. C. Activation of carboplatin by carbonate. *Chem. Res. Toxicol.* **2006**, *19*, 139–149.

(27) Tacka, K. A.; Dabrowiak, J. C.; Goodisman, J.; Penefsky, H. S.; Soid, A.-K. Effects of Cisplatin on mitochondrial function of Jurkat cells. *Chem. Res. Toxicol.* **2004**, *17*, 1102–1111.

and serves as a substrate for some intracellular caspases. Intracellular caspases cleave Ac-DEVD-AFC at the aspartate residue,<sup>28–30</sup> and this has been used<sup>29</sup> to measure caspase activity associated with apoptosis. In the present study, the resulting fluorescent AFC is determined quantitatively by HPLC analysis of cell lysates.

Many workers have studied the roles of different caspases in immunotoxin-induced<sup>31</sup> and drug-induced<sup>32–41</sup> apoptosis. However, with few exceptions,<sup>42,43</sup> the time-course of caspase activation has not been studied, nor has measured caspase activity been compared to measured respiration rate, ATP

(28) Nicholson, D. W.; Thornberry, N. A. Caspases: killer proteases. *Trends Biochem. Sci.* **1997**, *22*, 299–306.

(29) Gurtu, V.; Kain, S. R.; Zhang, G. Fluorometric and colorimetric detection of caspase activity associated with apoptosis. *Anal. Biochem.* **1997**, *251*, 98–102.

(30) Martins, L. M.; Kottke, T.; Mesner, P. W.; Basi, G. S.; Sinha, S.; Frigon, N.; et al. Activation of multiple interleukin-1beta converting enzyme homologues in cytosol and nuclei of HL-60 cells during etoposide-induced apoptosis. *J. Biol. Chem.* **1997**, *272*, 7421–7430.

(31) Keppler-Hafkemeyer, A.; Brinkmann, U.; Pastan, I. Role of caspases in immunotoxin-induced apoptosis of cancer cells. *Biochem.* **1998**, *37*, 16934–16942.

(32) Kim, W. H.; Yeo, M.; Kim, M. S.; Chun, S. B.; Shin, E. C.; Park, J. H.; Park, I. S. Role of caspase-3 in apoptosis of colon cancer cells induced by nonsteroidal anti-inflammatory drugs. *Int. J. Colorectal Dis.* **2000**, *15*, 112–113.

(33) Mese, H.; Sasaki, A.; Nakayama, S.; Alcalde, R. E.; Matusumura, T. The role of caspase family protease, caspase-3 on cisplatin-induced apoptosis in cisplatin-resistant A431 cell line. *Cancer Chemother. Pharmacol.* **2000**, *46*, 241–245.

(34) Xue, L.-Y.; Chiu, S.-M.; Oleinick, N. L. Photodynamic therapy-induced death of MCF-7 human breast cancer cells: a role for caspase-3 in the late step of apoptosis but not for the critical lethal event. *Exp. Cell Res.* **2001**, *263*, 145–155.

(35) Milner, A. E.; Palmer, D. H.; Hodgkin, E. A.; Eliopolous A. G.; Knox, P. G.; Poole, C. J.; Kerr, D. J.; Young, L. S. Induction of apoptosis by chemotherapeutic drugs: the role of FADD in activation of caspase-8 and synergy with death-receptor ligands in ovarian carcinoma cells. *Cell Death Differ.* **2002**, *9*, 287–300.

(36) Waltereit, R.; Weller, M. The role of caspases 9 and 9-short (9S) in death ligand- and drug-induced apoptosis in human astrocytoma cells. *Brain Res.: Mol. Brain Res.* **2002**, *106*, 42–49.

(37) Emanuele, S.; Calvaruso, G.; Lauricella, M.; Giuliano, M.; Bellavia, G.; D'Anneo, A.; Vento, R.; Tesoriere, G. Apoptosis induced in hepatoblastoma HepG2 cells by the proteosome inhibitor MG132 is associated with hydrogen peroxide production, expression of Bcl-XS and activation of caspase-3. *Int. J. Oncol.* **2002**, *21*, 857–865.

(38) Zhang, B.; Zhang, Y.; Shacter, E. Caspase 3-mediated inactivation of Rac GTPases promotes drug-induced apoptosis in human lymphoma cells. *Mol. Cell. Biol.* **2003**, *23*, 5716–5725.

(39) Zhao, X.; Tian, H.; Quan, P.; Liu, S. Correlation between drug resistance of leukemic cells and caspase-3. *Xi'an Jiaotong Daxue Xuebao, Yixueban* **2005**, *26*, 463–466.

(40) Loegering, D. A.; Ruchaud, S.; Earnshaw, W. C.; Kaufmann, S. H. Evaluation of the role of caspase-6 in anticancer drug-induced apoptosis. *Cell Death Differ.* **2006**, *13*, 346–347.

(41) Filomenko, R.; Prevotat, L.; Rebe, C.; Cortier, M.; Jeannin, J.-F.; Solary, E.; Bettaleb, A. Caspase-10 involvement in cytotoxic drug-induced apoptosis of tumor cells. *Oncogene* **2006**, *25*, 7635–7645.

level, or other measures of the progress of apoptosis. This study aimed to compare the time-dependency of intracellular caspase activation with that of the inhibition of cellular respiration. For the drugs and cells examined in this study, caspase activity was observed to remain low for hours, and then increase markedly (the “caspase storm”). A second aim was to determine if these time profiles differed for different cells and different drugs.

## Materials and Methods

**Chemicals.** Doxorubicin HCl (3.45 mM) was purchased from GensiaSicor Pharmaceuticals. Dactinomycin (actinomycin D, MW 1255.43) was purchased from Merck. Cisplatin (1 mg/mL, ~3.3 mM in 154 mM NaCl) was obtained from American Pharmaceutical Partners. Carboplatin (MW 371.25) was purchased as 26.9 mM solution (50 mg of carboplatin in 5 mL water) from Mayne Pharma (USA) Inc. Oxaliplatin (MW 397.3) was purchased as 12.5 mM solution (50 mg of oxaliplatin in 10 mL of dH<sub>2</sub>O) from Central Pharmacy. A lyophilized powder of caspase inhibitor I (zVAD-fmk, MW 467.5) was purchased from Calbiochem. Ac-DEVD-AFC (MW 729.6) and caspase-3 (molecular mass 30.5 kDa, heterodimer active human recombinant) were purchased from Axxora LLC. The remaining reagents were purchased from Sigma-Aldrich.

**Solutions.** Dactinomycin solution was made fresh in dH<sub>2</sub>O; its final concentration was determined by absorbance at 440 nm, using an extinction coefficient of 24 450 M<sup>-1</sup> cm<sup>-1</sup>. The zVAD-fmk solution (2.14 mM) was made by dissolving 1.0 mg of zVAD-fmk in 1.0 mL of dimethyl sulfoxide and stored at -20 °C. The nonfluorescent Ac-DEVD-AFC caspase substrate was dissolved in dimethyl sulfoxide at a final concentration of 6.85 mM and stored at -20 °C in small aliquots. Caspase-3 was dissolved at 5 µg per mL of 50 mM Tris-HEPES (pH 7.5) and stored at -70 °C in small aliquots.

**Cells.** Cells were cultured in RPMI-1640 supplemented with 10% fetal bovine serum as described.<sup>22</sup> The cell count and viability were determined by light microscopy, using a hemocytometer under standard trypan blue staining conditions.

**HPLC.** AFC was separated on HPLC in order to eliminate the fluorescent background present in the cell extracts. The analysis was performed on a Beckman reversed-phase HPLC system, which consisted of an automated injector (model 507e), a pump (model 125), and a fluorescent detector. The excitation wavelength was 400 nm and emission wavelength 505 nm. The solvent was HPLC-grade methanol. The

column, 4.6 × 250 mm Beckman Ultrasphere IP column, was operated at room temperature at a flow rate of 0.5 mL/min. The run time was 30 min. The injection volume was 10 µL.

PeakFit software (AISN Software) was utilized in the fitting of the HPLC AFC peaks. The Savitsky-Golay method was sometimes used to smooth the chromatogram before fitting a section of it to a sum of Gaussian peaks; this smoothing procedure did not affect the peak areas. Usually, four peaks were used in a fitting, of which the first and smallest was attributed to noise. The areas of the remaining peaks were summed up and counted as the total AFC peak area. The *R*<sup>2</sup> values in the fits varied from 0.754 to 0.996.

**Caspase-3 Activity in Solution.** Mixtures (final volume, 0.5 mL) containing 250 mM sucrose, 100 mM NaCl, 20 mM Tris-HEPES (pH 7.5), 10 mM dithiothreitol, 1 mM EDTA, Ac-DEVD-AFC, and caspase-3 (with and without 20 µM zVAD-fmk) were incubated at 37 °C for 15 min. Each sample was injected immediately into the HPLC at the end of the incubation period. The AFC peaks were detected by fluorescence and their areas were analyzed as described above.

**Intracellular Caspase Activity.** Cell suspensions containing 10<sup>6</sup> cells per mL in medium, 68 µM Ac-DEVD-AFC, and various concentrations of cytotoxic drugs (with and without 20 µM zVAD-fmk) were incubated at 37 °C. At the end of each incubation period, the suspension was immediately sonicated on ice for 60 s and then passed 10 times through 26-gauge needles. The cleavage reaction was quenched upon cell disruption, partly because caspases became inactive in the medium and partly because of dilution. The supernatants were collected by centrifugation (~12300g for 15 min), separated on HPLC, and analyzed for free AFC as described above.

Some experiments were performed with no substrate in the incubation solution. In these experiments, substrate was added to the solution at the end of the incubation period and incubation with substrate was carried out for 30 min before lysing the cells and analyzing for free AFC. These experiments showed that substrate enters cells rapidly. When substrate is present in solution from *t* = 0, the amount of AFC measured is the integral over incubation time of the rate of substrate cleavage since cleavage may occur from *t* = 0. When substrate is added only at the end of incubation, the amount of AFC measured is the cleavage rate multiplied by the time (30 min) during which substrate is present. The cleavage rate may be assumed to be constant over this time.

Each series of experiments was repeated at least three times, sometimes with cells from the same batch and sometimes with similar cells from a new batch. The values of the AFC peak areas after a given incubation time were not very reproducible between series because, in either case, the cells were not the same. However, the patterns, i.e., the variation of AFC peak areas with incubation time, were consistent between series.

(42) Johansson, A.-C.; Steen, H.; Ollinger, K.; Roberg, K. Cathepsin D mediates cytochrome c release and caspase activation in human fibroblast apoptosis induced by staurosporine. *Cell Death Differ.* **2003**, *10*, 1253–1259.  
(43) Huo, J. X.; Metz, S. A.; Li, G. D. p53-independent induction of p21(waf1/cip1) contributes to the activation of caspases in GTP-depletion-induced apoptosis of insulin-secreting cells. *Cell Death Differ.* **2004**, *11*, 99–109.

**Cleavage of Ac-DEVD-AFC.** The HPLC area ( $A$ ) corresponding to AFC is assumed to depend linearly on AFC concentration:

$$[S]_0 - [S] = [P] = aA + b \quad (1)$$

where  $[S]_0$  is the initial concentration of Ac-DEVD-AFC,  $[S]$  is the concentration after reaction, and  $[P]$  is the concentration of AFC. If  $A_t$  represents the total AFC area when all Ac-DEVD-AFC is consumed, i.e., when  $[S] = 0$ ,  $[S]_0 = aA_t + b$ . According to the Michaelis–Menten equation,

$$\frac{1}{V} = \frac{K_m}{V_{max}[S]} + \frac{1}{V_{max}}$$

where  $V = d[P]/dt = -d[S]/dt$ . The rate of change of AFC peak area  $V_{PA}$  is  $V/a$ . Noting that  $[S] \approx [S]_0$  in the initial period of the reaction, we have

$$\frac{1}{V_{PA}} = \frac{aK_m}{V_{max}[S]_0} + \frac{a}{V_{max}} \quad (2)$$

From the experimentally determined AFC peak areas, we obtain  $V_{PA} = A/T$ ,  $T = 15$  min (900 s), and plot  $1/V_{PA}$  vs  $1/[S]_0$ . Dividing the slope of the plot by the intercept, we obtain  $K_m$  in units of  $[S]_0$ ; it is not possible to obtain  $V_{max}$ , but only  $a/V_{max}$ .

**Oxygen Consumption.** Concentration of  $O_2$  in the cell suspensions was determined as a function of  $t$  at 37 °C using the phosphorescence of Pd(II) *meso*-tetra(4-sulfonatophenyl)-tetrabenzoporphyrin(Pd phosphor), as described.<sup>16</sup> The respiratory substrate was glucose. The rate of respiration was the negative slope of the curve of  $[O_2]$  vs  $t$  (zero-order rate constant,  $k$ , in  $\mu\text{M } O_2 \text{ min}^{-1}$  per  $10^6$  cells). Briefly, the samples (in sealed vials) were exposed to 10 flashes per second from a pulsed light-emitting diode array. Emitted phosphorescent light was detected by a photomultiplier tube after passing through a filter centered at 800 nm. The phosphorescence decay was a single exponential,  $I_0 e^{-t/\tau}$  with  $\tau^0/\tau = 1 + \tau^0 k_q [O_2]$ . Here,  $\tau$  is the lifetime in the presence of  $O_2$ ;  $\tau^0$ , the lifetime in the absence of  $O_2$ ;  $k_q$ , the second-order  $O_2$  quenching rate constant ( $96.1 \pm 1.2 \mu\text{M}^{-1} \text{ s}^{-1}$ ).<sup>16</sup>

**Cellular ATP Content.** Cellular ATP content was measured using the luciferin/luciferase bioluminescence system.<sup>16,17</sup> Cellular acid extracts were prepared by sonication of acid-treated cell protein on ice, followed by centrifugation and neutralization. The ATP content of the resulting supernatant was determined from the decay of luciferin bioluminescence. Luminescence was measured at 37 °C using a luminometer (Chrono-Log Corporation, Havertown, PA) connected to the Chrono-log AGGRO/LINK interface.

The luminometer was calibrated as follows: For known concentrations of ATP, plots of luminescence intensity  $I$  vs  $t$  were obtained, intensity being measured every 0.5 s out to 600 s. The plots were well fit to the two-parameter function,  $I = a e^{-bt}$ . We have shown that  $a$  is independent of [ATP], being a property of the luciferin/luciferase system, whereas

the parameter  $b$  should be proportional to [ATP] for small [ATP].<sup>17</sup> Our results for  $[ATP] \leq 0.2 \mu\text{M}$  are fit by  $b = 0.00467 \mu\text{M}^{-1} [\text{ATP}]$ ,  $r^2 = 0.984$ . It was important to recalibrate every new batch of luciferin–luciferase mixture.

## Results

**Caspase-3 Activity in Solution.** Caspase-3 activity with Ac-DEVD-AFC as substrate was first examined in a buffered solution. Typical chromatograms are shown in Figure 1A. The AFC peak areas of solutions containing caspase-3 and Ac-DEVD-AFC were linear with caspase-3 concentration ( $R^2 = 0.972$ ), Figure 1B. The AFC peak areas were also linear with time for the first 3 h of incubation ( $R^2 > 0.995$ ), but leveled off thereafter (Figure 1C). The AFC peak areas were likewise proportional ( $R^2 = 0.995$ ) to Ac-DEVD-AFC concentrations,  $[S]$ , up to  $[S] = 400 \mu\text{M}$ , obeying  $A = (304 \pm 371) + (113.9 \pm 2.4)[S]$ . The reaction rate did not become independent of [Ac-DEVD-AFC] until the concentration of the latter exceeded 1.0 mM. These results are displayed in the double-reciprocal plot of Figure 1D, where  $V_{PA}$  is the AFC peak area divided by the incubation time, 900 s. From this plot, we obtain ( $R^2 = 0.954$ ) a slope of  $6.34 \pm 0.35 \text{ s } \mu\text{M}^{-1}$  and an intercept of  $0.0078 \pm 0.0046 \text{ s}$ , so that  $K_m = 812 \pm 478 \mu\text{M}$ .

**Caspase Activation in Jurkat Cells.** We next investigated the cleavage of Ac-DEVD-AFC in Jurkat cells treated with dactinomycin and doxorubicin. Intracellular caspase activation was monitored as a function of time in the presence of 10 or 40  $\mu\text{M}$  dactinomycin (Figure 2A). Without the drug (circles), the AFC peak areas did not change over the 8 h incubation period. For cells incubated with 10  $\mu\text{M}$  dactinomycin (diamonds), there was no change in the AFC peak areas for the first 2 h; thereafter, the areas increased markedly, reflecting active caspases. After 4 h incubation, the AFC peak areas became essentially independent of incubation time. The variation of AFC peak area with time was found to be the same when 40  $\mu\text{M}$  dactinomycin was used (triangles), indicating that maximum caspase activation was reached with 10  $\mu\text{M}$  dactinomycin.

A linear increase in the AFC peak areas with time is indicative of a constant caspase activity since the velocity of the cleavage reaction is constant when the caspase activity is constant. In the experiments of Figure 2, we measured the total amount of cleavage during the incubation period. Thus, experiments in which AFC peak areas did not change with incubation time are indicative of zero caspase activity.

We next monitored caspase activation as a function of time in the presence of 20  $\mu\text{M}$  dactinomycin with and without zVAD-fmk (Figure 2B). With no drug (circles), the AFC peak areas remained at a constant low level for 8 h. With drug but without zVAD-fmk (diamonds), there was no increase in the AFC peak areas for 3 h, at which time the areas increased sharply, reaching a plateau at 7 h. These results were very similar to those of Figure 2A, confirming that 10  $\mu\text{M}$  drug produced the maximum effect. The presence

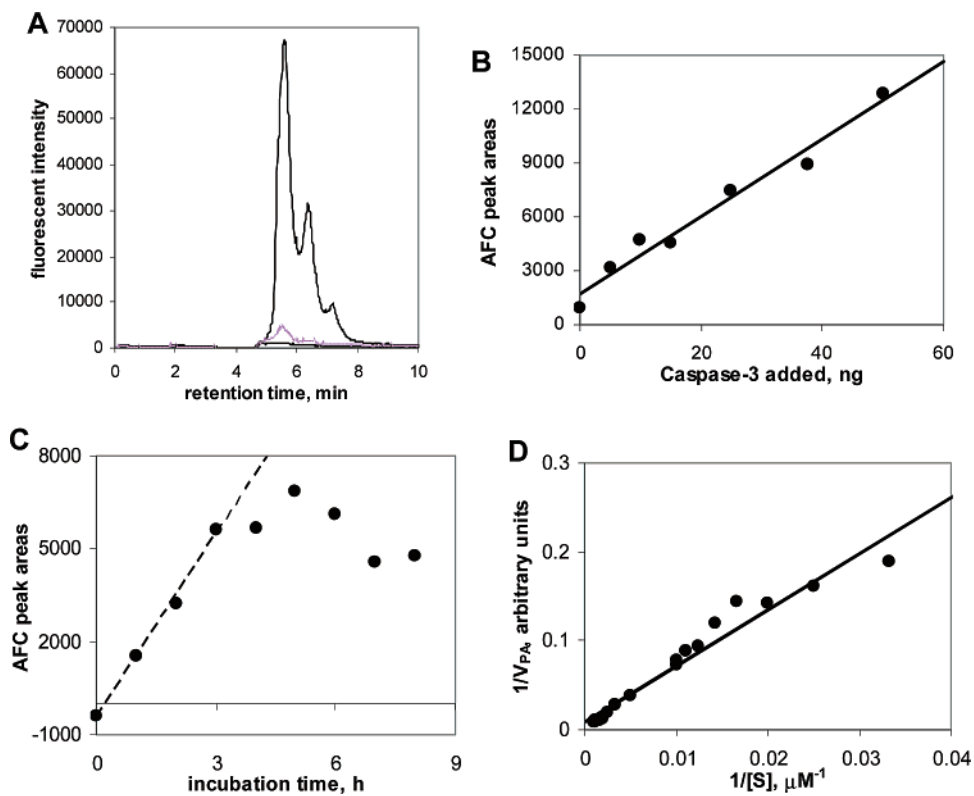


**Figure 1.** Caspase-3 activity in solution. Mixtures (final volume, 0.5 mL) containing 250 mM sucrose, 100 mM NaCl, 20 mM Tris-HEPES (pH 7.5), 10 mM dithiothreitol, 1 mM EDTA, Ac-DEVD-AFC, and caspase-3 (with and without 20  $\mu M$  zVAD-fmk) were incubated at 37 °C. (A) Representative HPLC chromatograms of the mixtures incubated with 25 ng of caspase-3 and 68  $\mu M$  Ac-DEVD-AFC at 37 °C for 1 h. The three plots, from bottom to top, are buffer + caspase-3; buffer + caspase-3 + Ac-DEVD-AFC + zVAD-fmk; and buffer + caspase-3 + Ac-DEVD-AFC. (B) The mixtures were incubated with 68  $\mu M$  Ac-DEVD-AFC and indicated amounts of caspase-3 for 1 h. These AFC peak areas were obtained by subtracting the peak area for the buffer (1264, in arbitrary units) from the peak areas for solutions containing Ac-DEVD-AFC and caspase-3. (C) The mixtures were incubated with 68  $\mu M$  Ac-DEVD-AFC and 25 ng of caspase-3 for indicated periods. These AFC peak areas were obtained by subtracting the peak area for solution containing buffer plus Ac-DEVD-AFC (6752, in arbitrary units) from the peak areas for solutions containing Ac-DEVD-AFC and caspase-3. (D) The mixtures were incubated with 25 ng of caspase-3 and indicated concentrations of Ac-DEVD-AFC for 15 min. The AFC peak areas were proportional to [Ac-DEVD-AFC] ( $R^2 = 0.995$ ) up to 400  $\mu M$ . Dividing peak areas by incubation time (900 s) gives the velocities  $V_{PA}$  (see eq 2), shown in the diagram as a double-reciprocal plot. From the slope and intercept we obtain  $K_m = \sim 812 \mu M$ .

of zVAD-fmk (triangles) completely abolished the formation of AFC, giving peak areas (triangles) even lower than with no drug.

We next evaluated the cleavage of Ac-DEVD-AFC in Jurkat cells treated with 10, 20, or 40  $\mu M$  doxorubicin (Figure 3). With no drug present (circles), the AFC peak areas did not change over the 8 h period (the slope of the best-fit line was  $23 \pm 86 \text{ h}^{-1}$ , i.e., zero). In the presence of 10, 20, or 40  $\mu M$  doxorubicin (squares, diamonds, and triangles, respectively), the AFC peak areas increased after 2 h, reflecting caspase activity. For the three concentrations, the AFC peak areas reached a limiting value at 7 h, similar to experiments with dactinomycin. There was little difference in the results obtained with 10, 20, or 40  $\mu M$  doxorubicin (it should be noted that the batch of cells for the 20  $\mu M$  experiment was different from the others).

The effect of zVAD-fmk on intracellular caspase activation is shown in Figure 3B. For untreated cells (circles), caspase activity was negligible for 8 h (the slope of the best-fit dashed

line was  $203 \pm 95 \text{ h}^{-1}$ , i.e., zero). With 20  $\mu M$  doxorubicin (squares), the AFC peak areas were linear with time between 3 h and 7 h. With the addition of 20  $\mu M$  zVAD-fmk as well as 20  $\mu M$  doxorubicin (triangles), the AFC peak areas were reduced to the level for no drug and were independent of time (the slope of the best-fit solid line was  $-64 \pm 86 \text{ h}^{-1}$ , i.e., zero). Thus, zVAD-fmk again completely abolished the intracellular cleavage of Ac-DEVD-AFC.

It is possible that the approximately 2 h delay in the development of caspase activity (Figures 2 and 3) was due to a slow influx of Ac-DEVD-AFC into the cells. We performed the following experiment to determine if cleavage of Ac-DEVD-AFC occurs immediately in cells with active caspases. Jurkat cells were exposed to 20  $\mu M$  doxorubicin for 3 h at 37 °C (under these conditions active intracellular caspases are present). Ac-DEVD-AFC (68  $\mu M$ ) was then added to the solution. Cell samples were taken every 5 min from  $t = 180$  min to 215 min (the addition of Ac-DEVD-AFC was made at  $t = 180$  min), every 10 min to 240 min,

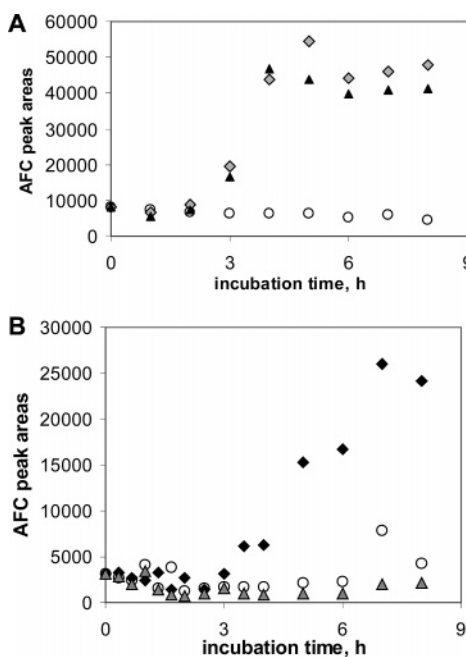


**Figure 2.** Intracellular caspase activation by dactinomycin in Jurkat cells. (A) Jurkat cell suspensions containing  $10^6$  cells/mL in medium, 68  $\mu$ M Ac-DEVD-AFC, and 10 or 40  $\mu$ M dactinomycin were incubated at 37 °C for 8 h. Circles, no drug; diamonds, 10  $\mu$ M drug; triangles, 40  $\mu$ M drug. (B) Jurkat cells ( $10^6$  cells/mL) were incubated with 20  $\mu$ M dactinomycin with and without 20  $\mu$ M zVAD-fmk. Circles, no drug; diamonds, dactinomycin; triangles, dactinomycin + zVAD-fmk.

and every hour thereafter, and analyzed for AFC. After subtraction of the peak area for  $t = 0$  (beginning of incubation) from all measured areas, the results of Figure 4A were obtained.

There was a linear increase in the AFC peak areas between  $t = 200$  min (i.e., within 20 min of addition of Ac-DEVD-AFC) and  $t = 420$  min ( $R^2 = 0.9588$ ), as shown by the dashed line, corresponding to the level of caspase activity existing after 3 h incubation. Also, the peak intensity at  $t = 180$  min was higher for treated than for untreated cells, just as in Figures 2 and 3. These observations support the conclusion that cellular influx of the substrate was not rate limiting. The results also show that intracellular caspase activity reached a constant value by 3 h, giving a constant rate of cleavage of Ac-DEVD-AFC and linearly increasing amounts of AFC with  $t$  (Figure 4A).

Because Ac-DEVD-AFC enters cells rapidly, it was possible to design an experiment that could determine the intracellular caspase activity at a particular time, rather than the cumulative substrate cleavage. Cell suspensions were incubated with and without 20  $\mu$ M dactinomycin or 20  $\mu$ M doxorubicin at 37 °C, with no Ac-DEVD-AFC present. At the end of each incubation period, Ac-DEVD-AFC was added and the incubation was continued at 37 °C for an additional 30 min. The resulting AFC peak areas are shown in Figure 4B. For both doxorubicin and dactinomycin, the cleavage remained low before 3 h incubation time, increased (slowly at first) between 3 h and 6 h, and decreased after

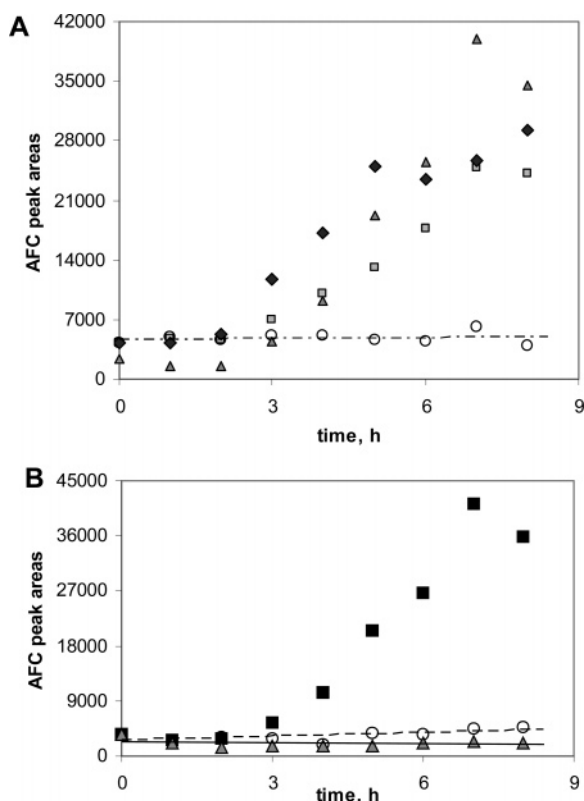


**Figure 3.** Intracellular caspase activation by doxorubicin in Jurkat cells. (A) Jurkat cell suspensions containing  $10^6$  cells/mL in medium, 68  $\mu$ M Ac-DEVD-AFC, and doxorubicin were incubated at 37 °C for 8 h. Circles, no drug; squares, 10  $\mu$ M drug; triangles, 20  $\mu$ M drug; diamonds, 40  $\mu$ M drug. (B) Jurkat cells ( $10^6$  cells/mL) were incubated with 20  $\mu$ M doxorubicin with and without 20  $\mu$ M zVAD-fmk. Circles, no drug; diamonds, doxorubicin; triangles, doxorubicin + zVAD-fmk.

~8 h (a “storm-like” pattern). It is not clear whether the decline in the caspase activity after 8 h was due to caspase leakage, caspase decay, ATP depletion, or cell death. It should be noted that cell viability during the time course of drug treatment remained almost unchanged.

The areas of Figure 4B for doxorubicin, for  $t$  from 3 to 7 h, were well fit ( $R^2 = 0.9837$ ) to a line with the equation  $A = 2320 + 5817(t - 2.5)$ ; the origin of caspases was arbitrarily set at 2.5 h. (The areas obtained with dactinomycin exhibited too much scatter for a meaningful calculation.) Dividing by 1/2 h (time of incubation with substrate) gave the rate,  $dA/dt$ . Integrating  $dA/dt$  from 2.5 h gave the areas that should be obtained from a continuous incubation with doxorubicin and Ac-DEVD-AFC, such as those shown in Figure 2B.

$$\int_{2.5}^t [4640 + 11634(t - 2.5)] dt =$$

$$4640(t - 2.5) + 11634 \frac{(t - 2.5)^2}{2}$$

The first term reflects caspase activity present before 2.5 h and was neglected. For  $t = 3, 4$ , and 5 h, the second term gave areas of 1454, 13 088, and 36 356, respectively. These

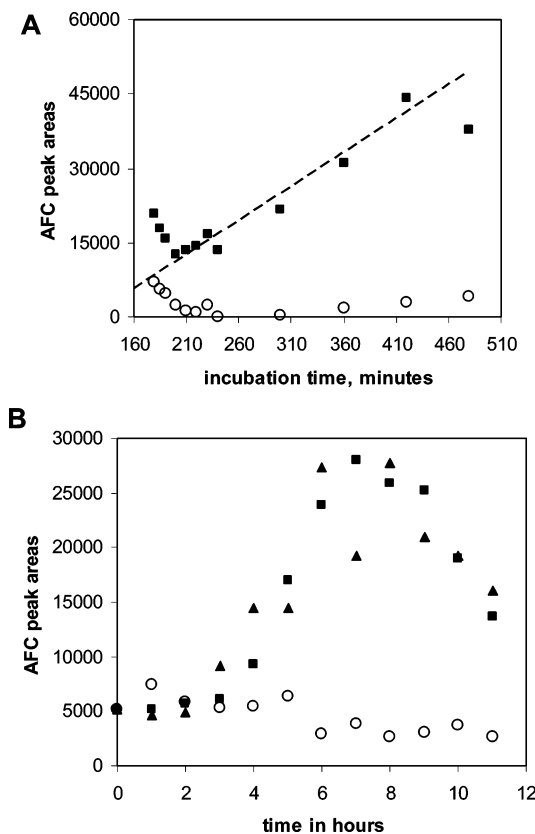


**Figure 4.** Caspase activity in Jurkat cells. (A) The cell suspensions ( $10^6$  cells/mL medium) were incubated with  $20 \mu\text{M}$  doxorubicin at  $37^\circ\text{C}$  for 3 h. Ac-DEVD-AFC ( $68 \mu\text{M}$ ) was then added and the incubation continued for indicated periods. Measurements were made every 10 min starting at 180 min, the time of addition of Ac-DEVD-AFC. Circles, no drug; squares, with doxorubicin; dashed line, linear fit to points for  $t = 200$ – $420$  min ( $R^2 = 0.9588$ ). (B) The cell suspensions ( $10^6$  cells/mL medium) were incubated with and without  $20 \mu\text{M}$  dactinomycin or  $20 \mu\text{M}$  doxorubicin at  $37^\circ\text{C}$ . At the end of each incubation period, 1.0 mL of each suspension was removed and incubated with  $68 \mu\text{M}$  Ac-DEVD-AFC at  $37^\circ\text{C}$  for an additional 30 min. Circles, no drug; squares, doxorubicin; triangles, dactinomycin.

values were in rough agreement with the corresponding areas in Figure 3B: 5514, 10 286, and 20 415, respectively. These results show consistency between the types of experiments in Figures 2 and 3 and that in Figure 4B.

Since caspase activation during apoptosis is accompanied by decreased respiration and ATP depletion,<sup>16,17</sup> we measured respiration and ATP levels in Jurkat cells incubated with dactinomycin or doxorubicin. The rate of respiration ( $k$ , in  $\mu\text{M O}_2 \text{ min}^{-1}$  per  $10^6$  cells) was obtained from the negative of the slope of the curve of  $[\text{O}_2]$  vs  $t$  for a sample in a sealed vial, such as the curves shown in Figure 5A. Jurkat cells were incubated in medium at  $37^\circ\text{C}$  with or without  $20 \mu\text{M}$  doxorubicin or dactinomycin. Every hour, a sample was placed in a sealed vial for oxygen measurement (with  $t = 0$  corresponding to the addition of drug). The values of  $k$  obtained from these series are plotted in Figure 5B. In untreated cells (circles), the rate of respiration increased,

probably due to cell growth. With dactinomycin (triangles) or doxorubicin (squares), the rate of respiration rate was constant (dactinomycin) or slightly increased (doxorubicin) during the first 5 h and then decreased gradually. At all times, the values of  $k$  were lower for dactinomycin-treated cells than for doxorubicin-treated cells.

Simultaneously with the samples taken for measurement of respiration, samples were taken for measurement of ATP content. The average of the results obtained is shown in Figure 5C as a function of incubation time, with standard deviation ( $n = 3$ ). The ATP content in untreated Jurkat cells remained essentially constant for incubation times up to 11 h (slope =  $-0.31 \pm 0.19 \text{ nmol h}^{-1}$  per  $10^6$  cells). Cellular ATP in doxorubicin- or dactinomycin-treated cells (squares and triangles, respectively) remained constant for the first 4 h, and then decreased with incubation time until nearly complete depletion at 9 h.

**Effect of Pt Drugs on Caspase Activity.** We then studied the effects of Pt drugs (cisplatin, carboplatin, and oxaliplatin) on caspase activation in Jurkat cells. Cisplatin has been shown to diminish cellular respiration after many hours of drug treatment.<sup>22</sup> In these experiments, cell suspensions ( $10^6$  cells/mL) in medium including  $68 \mu\text{M}$  Ac-DEVD-AFC were incubated for up to 22 h at  $37^\circ\text{C}$ . The following conditions were included: no added drug;  $20 \mu\text{M}$  cisplatin, carboplatin, or oxaliplatin;  $20 \mu\text{M}$  cisplatin, carboplatin, or oxaliplatin plus  $20 \mu\text{M}$  zVAD-fmk. Samples were taken every 2 h and analyzed for caspase activity. The AFC peak areas are shown in Figure 6A–C. With no drug (circles), the AFC peak areas remained at a low level for 22 h, increasing slightly (slope =  $464 \pm 82 \text{ h}^{-1}$ ). With cisplatin but no zVAD-fmk (Figure 6A, black squares), the increase in the AFC peak areas was equal to that for untreated cells for the first 12 h (slope =  $351 \pm 109 \text{ h}^{-1}$ ). Subsequently, caspase activity rose more rapidly. With zVAD-fmk present in addition to cisplatin (Figure 6A, gray squares), caspase activity was reduced to a small value independent of time (slope =  $52 \pm 49 \text{ h}^{-1}$ ).

For carboplatin, which is clinically used at much higher doses than cisplatin, caspase levels in treated cells were similar to untreated cells up to 22 h (Figure 6B). The AFC peak areas for untreated cells obeyed  $(3523 \pm 1066) + (464 \pm 82)t$ , and for carboplatin-treated cells the areas obeyed  $(2750 \pm 813) + (520 \pm 63)t$ . With zVAD-fmk present, the areas were almost constant, obeying  $(3299 \pm 735) + (39 \pm 57)t$ .

The results for oxaliplatin were similar (Figure 6C). The AFC peak areas for oxaliplatin-treated cells obeyed  $(2101 \pm 1649) + (443 \pm 133)t$ , and peak areas for cells treated with oxaliplatin plus zVAD-fmk obeyed  $(2805 \pm 1475) + (161 \pm 119)t$ . The difference between the time profiles of caspase activation for different Pt drugs may be due to the stable ring structure in carboplatin and oxaliplatin. Ring opening is a necessary prerequisite for drug action.<sup>23</sup>

**Caspase Activation in HL-60/MX2 Cells.** HL-60/MX2 cells are resistant to doxorubicin because of their altered topoisomerase-II activity.<sup>18</sup> We compared caspase activation in HL-60/MX2 cells by doxorubicin to activation by

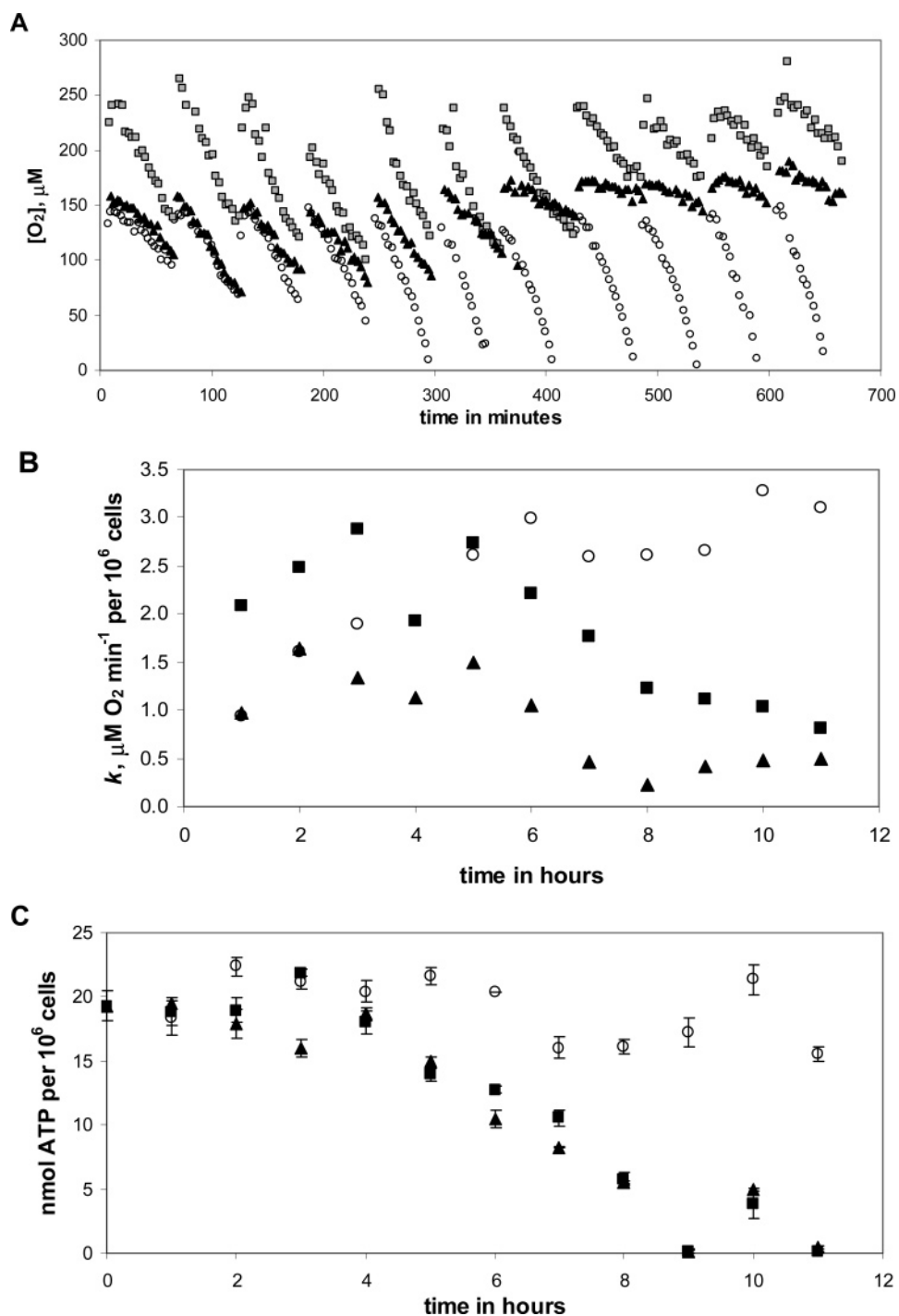


**Figure 5.** Cellular respiration injury and ATP damage in Jurkat cells by doxorubicin and dactinomycin. Jurkat cells were suspended at 37 °C with  $10^6$  cells/mL media, 10% fetal bovine serum, 2  $\mu M$  Pd phosphor, and 1% albumin. Three conditions were tested: without drug, with 20  $\mu M$  doxorubicin, and with 20  $\mu M$  dactinomycin. Every hour, samples (1.0 mL) from each cell suspension were placed in 1 mL glass vials, which were sealed and placed in the instrument for  $[O_2]$  measurements. (A) Measured  $[O_2]$  vs  $t$ . Minute zero corresponds to the addition of doxorubicin or dactinomycin. Circles, untreated cells; squares, cells treated with doxorubicin; triangles, cells treated with dactinomycin. (B) Absolute values of  $k$  determined by best-fit line to the results of (A). Circles, untreated cells; squares, cells treated with doxorubicin; triangles, cells treated with dactinomycin. Doxorubicin produced a sudden, and dactinomycin a more gradual, decrease in respiration with time. (C) Cellular ATP levels, in nmol of ATP/ $10^6$  Jurkat cells, as functions of incubation time. Circles, untreated cells; squares, cells treated with 20  $\mu M$  doxorubicin; triangles, cells treated with 20  $\mu M$  dactinomycin. With no drug, ATP level is constant over 11 h. With either drug, ATP level decreases gradually with  $t$ .

dactinomycin (whose activity is independent of topoisomerase-II). Smoothed HPLC chromatograms, for 3 h

incubation, are shown in Figure 7A,B. Figure 7A shows results for HL-60/MX2 cells incubated with no drug (light

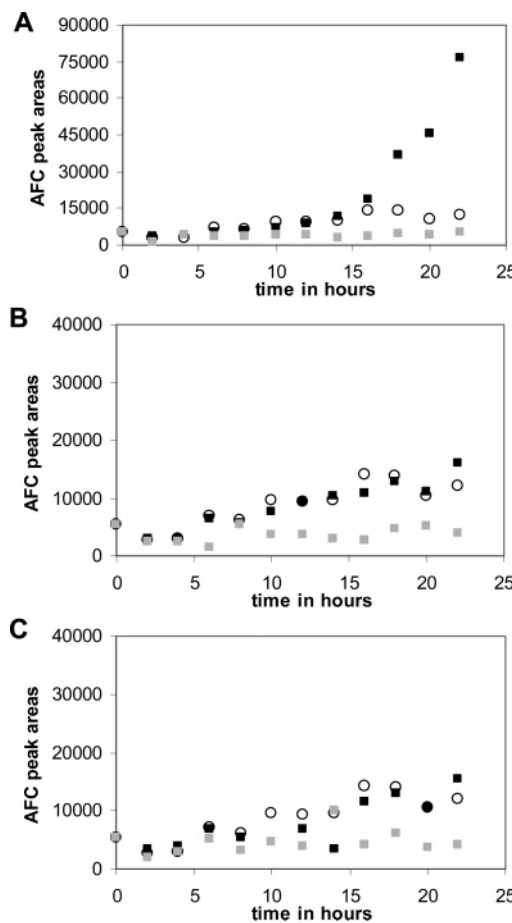


**Figure 6.** Caspase activation in Jurkat cells by Pt drugs. Cell suspensions ( $10^6$  cells/mL medium) containing  $68 \mu\text{M}$  Ac-DEVD-AFC, with and without  $20 \mu\text{M}$  Pt drug and with and without  $20 \mu\text{M}$  zVAD-fmk, were incubated for up to 22 h at  $37^\circ\text{C}$ . Samples were taken every 2 h and analyzed for caspase activity. (A) Cisplatin: circles, no drug; black squares, with drug; gray squares, with drug plus zVAD-fmk. (B) Carboplatin: circles, no drug; black squares, with drug; gray squares, with drug plus zVAD-fmk. (C) Oxaliplatin: circles, no drug; black squares, with drug; gray squares, with drug plus zVAD-fmk.

trace), with  $20 \mu\text{M}$  doxorubicin (dotted trace), and with  $20 \mu\text{M}$  dactinomycin (heavy trace). For comparison, the corresponding traces obtained with ordinary HL-60 cells are shown in Figure 7B.

Figure 7C shows the AFC peak areas obtained for HL-60/MX2 cells corresponding to the five conditions: untreated, treated with  $20 \mu\text{M}$  doxorubicin, treated with  $20 \mu\text{M}$  dactinomycin, treated with  $20 \mu\text{M}$  doxorubicin plus  $20 \mu\text{M}$  zVAD-fmk, and treated with  $20 \mu\text{M}$  dactinomycin plus  $20 \mu\text{M}$  zVAD-fmk. With no drug present (circles), the AFC peak areas did not significantly change over the 8 h period (the slope of the best-fit line, shown dashed in Figure 7C, was  $-432 \pm 205 \text{ h}^{-1}$ ). In the presence of  $20 \mu\text{M}$  doxorubicin (gray squares), a small increase in the AFC peak areas was first noticeable at 4 h. In the presence of  $20 \mu\text{M}$  dactinomycin (black diamonds), increases in the AFC peak areas appeared significantly earlier (at 3 h) and were larger than for

doxorubicin, except for  $t = 8$  h. In the presence of doxorubicin + zVAD-fmk (X's in squares), or dactinomycin + zVAD-fmk (gray diamonds), the AFC peak areas were lower than with no drug and did not change significantly with incubation time. The slopes of the best-fit lines for these areas vs  $t$  were, respectively,  $-249 \pm 166$  and  $-424 \pm 185 \text{ h}^{-1}$ .

For comparison, the same measurements were carried out on HL-60 cells, with intact topoisomerase-II (results not shown). For untreated cells, the AFC peak areas were much lower than for treated cells over the 8 h incubation period. For cells treated with  $20 \mu\text{M}$  doxorubicin or  $20 \mu\text{M}$  dactinomycin, the AFC peak areas were the same for either drug. For cells incubated with doxorubicin + zVAD-fmk or dactinomycin + zVAD-fmk, the AFC peak areas were lower than with no drug. Thus, in HL-60 cells, caspase activation by doxorubicin was similar to activation by dactinomycin.

Measurements of cellular respiration and ATP levels were carried out in order to confirm the differences between the effects of doxorubicin and dactinomycin on HL-60/MX2 cells. Suspensions of  $10^6$  cells per mL were incubated with no drug, with  $20 \mu\text{M}$  doxorubicin, or with  $20 \mu\text{M}$  dactinomycin for up to 11 h. Every hour, samples were removed for oxygen and ATP measurements. The slopes of  $[\text{O}_2]$ -vs- $t$  plots gave the respiration rates,  $k$ , which were then plotted vs incubation time in Figure 8A. The circles, corresponding to untreated cells, showed a progressive increase in oxygen consumption for 5 h of incubation time, probably due to cell growth, after which  $k$  became constant at about  $3 \mu\text{M O}_2 \text{ min}^{-1}$  per  $10^6$  cells. Cells treated with doxorubicin (squares) or dactinomycin (triangles) also showed an initial increase in oxygen consumption, but only for 3 h. For doxorubicin-treated cells, the values of  $k$  leveled off at 3 h, then dropped precipitously at 6 h, remaining constant (about  $1 \mu\text{M O}_2 \text{ min}^{-1}$  per  $10^6$  cells) thereafter. The effect of dactinomycin on respiration was more rapid;  $k$  started to decrease after 3 h incubation and continued to decrease thereafter, reaching  $\sim 1 \mu\text{M O}_2 \text{ min}^{-1}$  per  $10^6$  cells after 8 h. The difference between the drugs is consistent with the lack of topoisomerase-II, which is required for induction of apoptosis by doxorubicin, but not for induction by dactinomycin. The decrease in the values of  $k$  after 5 h for doxorubicin-treated cells suggests that alternative pathways may have executed the apoptosis.

Figure 8B shows the decreases in levels of ATP measured in cell samples removed from the incubation mixture every hour. Each of the ATP levels shown represents the average of three measurements. In Figure 8B, the ratio of [ATP] for treated cells to [ATP] for untreated cells is shown, with standard error derived from the standard deviations in both sets of measurements. Both drugs (squares = doxorubicin-treated cells, triangles = dactinomycin-treated cells) decrease ATP levels relative to untreated cells, with levels becoming relatively constant after 5 h. Dactinomycin is more effective in decreasing [ATP] than doxorubicin. Considering only results for  $t > 5$  h, the ratio of [ATP] in treated cells to [ATP] in untreated cells is  $0.70 \pm 0.20$  for doxorubicin and  $0.49 \pm$

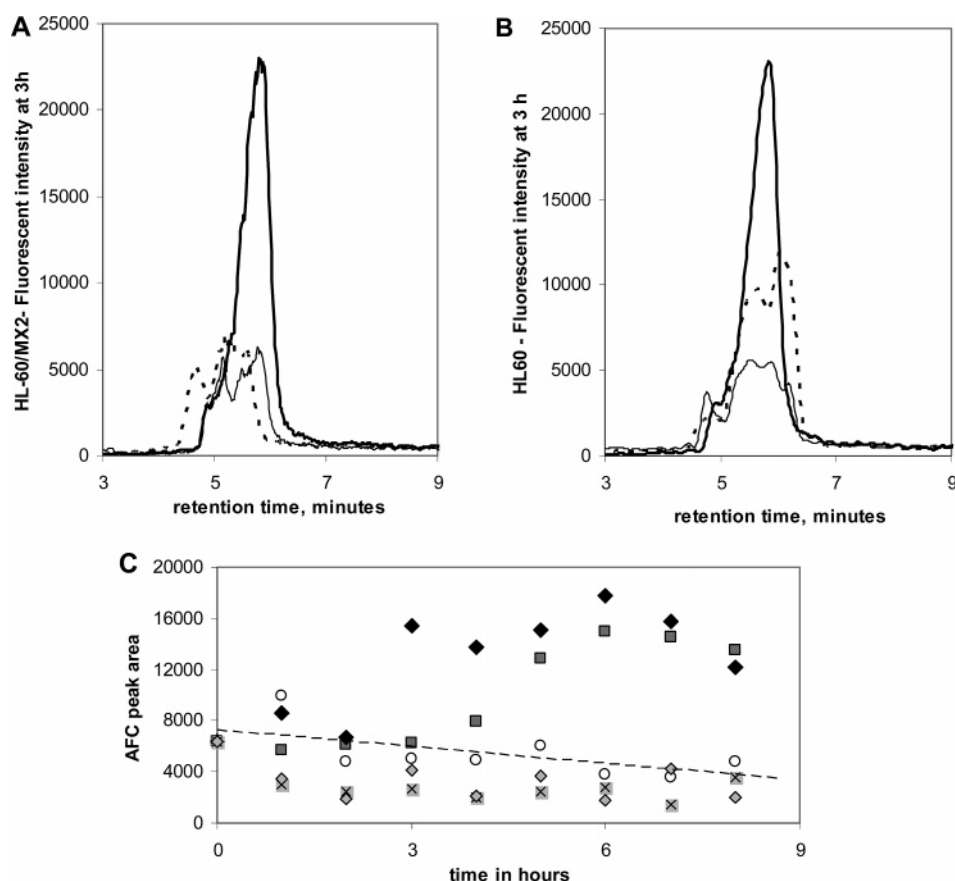


**Figure 7.** Caspase activation in HL-60/MX2 cells by dactinomycin and doxorubicin. Cell suspensions ( $10^6$  cells/mL medium) were incubated with  $68 \mu\text{M}$  Ac-DEVD-AFC and  $20 \mu\text{M}$  drug, with or without  $20 \mu\text{M}$  zVAD-fmk, at  $37^\circ\text{C}$ . Representative (smoothed) HPLC chromatographs at 3 h incubation are shown for (A) HL-60/MX2 and (B) HL-60 cells. Traces are for cells incubated with no drug (light line), with doxorubicin (dotted line), or with dactinomycin (dark line). (C) AFC peak areas for cells incubated with no drug (open circles), doxorubicin (gray squares), doxorubicin + zVAD-fmk (X's in squares), dactinomycin (black diamonds), or dactinomycin + zVAD-fmk (gray diamonds) for up to 8 h. Dashed line is linear fit to results for untreated cells, with slope =  $-432 \pm 205$ .

0.14 for dactinomycin. Thus doxorubicin and dactinomycin treatments reduce the ATP level by 30% and 51%, respectively.

## Discussion

We monitored intracellular caspase activation as a function of time during continuous exposure of cells to dactinomycin, doxorubicin, or Pt drugs. Caspase activity was measured using, as a reporter, the caspase-dependent formation of fluorescent AFC from Ac-DEVD-AFC.<sup>29,30</sup> We showed that Ac-DEVD-AFC rapidly enters the cell (Figure 4A,B). It is known to be efficiently cleaved by caspase-3 ( $k_{\text{cat}}/K_m$ ,  $1.3 \times 10^6 \text{ M}^{-1} \text{ s}^{-1}$ ) and caspase-7 ( $k_{\text{cat}}/K_m$ ,  $1.3 \times 10^4 \text{ M}^{-1} \text{ s}^{-1}$ ),<sup>29</sup> releasing AFC. After HPLC separation to remove interfering fluorescent substances in the cell extracts, AFC was detected by its fluorescence with great sensitivity. The AFC peak areas (typical chromatograms are shown in Figures 1A and 7A,B) are proportional to caspase activity as shown (Figure 1B).

In most of the experiments described, cells were incubated with the caspase substrate Ac-DEVD-AFC for a desired period of time. Cells were then lysed and cell contents were

analyzed for free AFC, produced by intracellular caspase-induced cleavage of the substrate. The pancaspase inhibitor zVAD-fmk completely blocked the appearance of the AFC peaks (Figures 2B, 3B, and 6), confirming that cleavage is mediated by cysteinyl proteases (caspases). In these experiments, the amount of AFC detected is proportional to the integral of the caspase level over incubation time. For example, the results for dactinomycin-treated Jurkat cells (Figure 2A) show that caspase activity is low during the first 2 h of incubation, but rises sharply thereafter. Since the amount of AFC levels off after  $\sim 4\text{--}5$  h, and we observe the total cleavage integrated over incubation time, this indicates that no further cleavage occurs after about 4 h.

The implication is that caspase activities drop to low values at 4 h, either because the caspases are inactivated or the cell membrane becomes leaky and the caspases escape. It is likely that drug-induced apoptosis has proceeded sufficiently so the cells are no longer viable after 4–5 h of incubation with dactinomycin. Results with  $20 \mu\text{M}$  doxorubicin (Figure 3) are similar to results with dactinomycin at the same concentration. However, the onset of caspase activity occurs

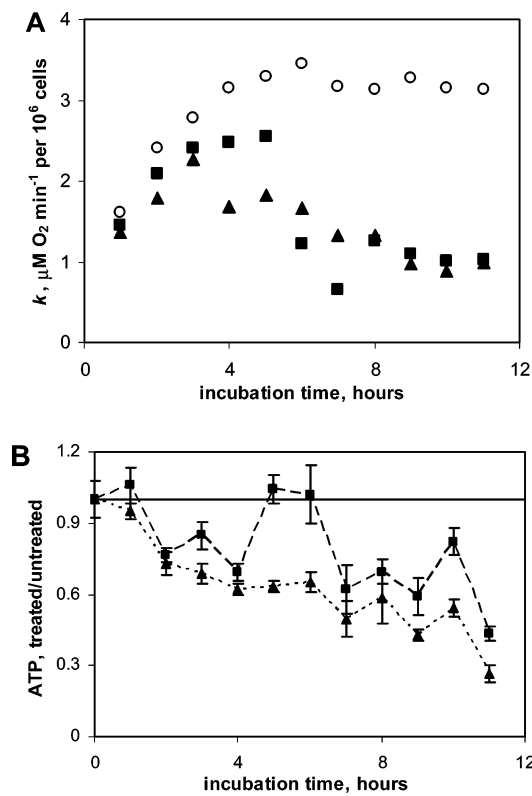


**Figure 8.** Respiration rate and ATP level in HL-60 cells treated with drug. Cell suspensions ( $10^6$  cells per mL of medium) were incubated with and without  $20 \mu\text{M}$  doxorubicin or dactinomycin at  $37^\circ\text{C}$  for 11 h. Every hour, samples were removed for measurement of oxygen consumption and ATP levels. (A) Samples were placed in sealed vials for measurement of  $[\text{O}_2]$  vs  $t$ . Respiration rate  $k$  was the slope of the  $[\text{O}_2]$ -vs- $t$  plot. Circles, untreated cells; squares, doxorubicin-treated cells; triangles, dactinomycin-treated cells. (B) Cells were lysed and  $[\text{ATP}]$  was measured immediately. The ratio of  $[\text{ATP}]$  in treated cells to  $[\text{ATP}]$  for untreated cells is plotted, with error bars calculated from the standard deviations of three measurements of treated and untreated cells. Squares, doxorubicin-treated cells; triangles, dactinomycin-treated cells.

at a slightly later time for doxorubicin and the disappearance of caspase activity, evidenced by the leveling-off in AFC peak areas, occurs after 6 h, rather than 4 h.

In order to measure directly the variation of caspase activity with time, we carried out several experiments in which substrate was not present during incubation of cells with drug. Substrate was added after the desired incubation period, and incubation continued for 30 min. The amount of cleavage was then proportional to the caspase activity during this 30 min period. The results of Figure 4B, obtained in this way, clearly show the onset of caspase activity at  $\sim 3$  h and the subsequent decline after about 8 h (a “storm-like” pattern).

The variation of caspase activity with time, as measured by the hydrolysis of Ac-DEVD-AFC, is paralleled by the observed time course of changes in cellular respiration and ATP content. The data in Figure 5A,B show that the decrease in respiration rate ( $k$ ) for cells treated with doxorubicin and

dactinomycin occurs after 4 h of incubation. Other experiments show that Jurkat cells incubated with doxorubicin exhibit almost the same values of  $k$  as untreated cells for several hours, after which  $k$  takes on a lower value.<sup>16</sup> In contrast, the values of  $k$  for dactinomycin-treated cells decrease gradually from the earliest times.<sup>17</sup> The data of Figure 5B are not precise enough to show clearly the distinction between the two drugs (concentrations and incubation times were different in the previous experiments).<sup>16,17</sup> Figure 5C shows that ATP levels are unaffected for 4 h with either drug. After 4 h, there is an essentially linear decrease in ATP level, which reaches zero at about 9 h. At this time,  $k$  has reached a constant value with dactinomycin, and its value with doxorubicin, while slightly higher, is decreasing only slightly. The value of  $k$  found for dactinomycin is approximately the same as that observed with cyanide-treated cells.<sup>17</sup>

By comparison, the effects of the three Pt drugs, cisplatin, carboplatin, and oxaliplatin, all at  $20 \mu\text{M}$ , were much different (Figure 6). It has been established<sup>33</sup> that activation of caspases, particularly caspase-3, can mediate apoptosis induced by cisplatin, even in cisplatin-resistant cells. We have previously shown<sup>22</sup> that cisplatin does not affect cellular respiration until at least 12 h after drug treatment. The present study shows that Jurkat cells incubated with cisplatin show a significant caspase activation only after 14 h. This is so in spite of the fact that the cells remain in continuous contact with the drug, unlike in our previous experiments<sup>22,27</sup> in which drug was removed after 2 h and cells were maintained in drug-free medium thereafter. At about 15 h of incubation with drug, caspase activities rise sharply in a similar “storm-like” pattern (Figure 6A).

With carboplatin and oxaliplatin, caspase activation was not observed, even at 22 h. It is possible that, with these drugs, caspase activation and impaired respiration occur at later times. The long delay observed for the effects of Pt drugs suggests that the mechanism of induction of apoptosis by these agents may differ from that for induction by the other drugs tested. However, the fact that an increase in caspase activity and a decrease in respiration occurred at about the same time, although that time was different for different drugs, indicates that the two processes are closely related in drug-induced apoptosis. If one of the processes is the cause of the other, the intermediate steps must be very rapid.

Doxorubicin and dactinomycin appear to act similarly in HL-60 cells and Jurkat cells. Caspase activities remain low during the first 2 to 3 h of drug treatment, after which they increase. A striking difference between the two drugs appears when the resistant HL-60/MX2 cells, which lack topoisomerase-II, are used (Figure 7C). Whereas dactinomycin induces a rapid increase in caspase activity at 3 h, doxorubicin causes an increase which is apparent only after 4 h, and is much more gradual. The dactinomycin-induced caspase activity appears to be complete at 4 h, at which time doxorubicin-induced caspase activity is still rising. For both drugs, AFC peak areas decrease after 6 h, but this is probably

a consequence of events occurring after apoptosis has progressed beyond the point of cell viability.

Caspase activation in cells exposed to dactinomycin and doxorubicin is very similar, occurring after  $\sim 2$  h of incubation and increasing linearly with time for 1–2 h, after which the concentration of the enzymes becomes constant for several hours. Although the plots of AFC peak areas vs  $t$  for dactinomycin and doxorubicin are similar (Figures 2–3), there are subtle differences between them. Dactinomycin is the more potent drug, with the maximum caspase activation occurring at  $10 \mu\text{M}$  (Figure 3A vs 4A). More importantly, dactinomycin is more effective than doxorubicin in HL-60/MX2 cells (Figure 7A,B), because action of the latter drug depends on topoisomerase-II, deficient in this cell line. However, despite the lack of topoisomerase-II activity, and the important role it plays in mediating sensitivity to doxorubicin, a prolonged exposure to doxorubicin eventually activates the caspases in these cells (Figure 7C). Consistently, caspase activation during etoposide-induced apoptosis in HL-60 cells shows that the pro-caspase-3 levels diminish 2–3 h after etoposide addition ( $68 \mu\text{M}$ ), and the cytosolic protease activity that cleaves Ac-DEVD-AFC increases 100-fold.<sup>30</sup>

Caspase activation in cells exposed to cisplatin occurs after  $\sim 14$  h of incubation, and the concentration of the enzymes becomes constant after  $\sim 16$  h. For the other platinum drugs, caspase activation is delayed even further. Mitochondrial dysfunction also occurred only after more than 12 h of incubation with Pt drugs. The differences in the reactivities among the three Pt drugs demonstrate a large influence of the ligands occupying the Pt coordination sphere. Steric hindrance may well explain the slow reactivity of carboplatin. The six-membered ring formed between the Pt and the bidentate ligand (1,1-cyclobutanedicarboxylato) of carboplatin adopts a configuration that forces the cyclobutane moiety to reside in an axial position of the Pt coordination sphere, preventing the nucleophile from reaching the Pt(II). The strain in the five-membered ring of oxaliplatin, on the other hand, is rapidly relieved by thiolate attack on Pt(II).

(44) Deveraux, Q. L.; Takahashi, R.; Salvesen, G. S.; Reed, J. C. X-linked IAP is a direct inhibitor of cell-death proteases. *Nature* **1997**, *388*, 300–304.

(45) Klock, R. M.; Bossy-Wetzel, E.; Green, D. R.; Newmeyer, D. D. The release of cytochrome *c* from mitochondria: a primary site for Bcl-2 regulation of apoptosis. *Science* **1997**, *275*, 1132–1136.

(46) Ricci, J.-E.; Gottlieb, R. A.; Green, D. R. Caspase-mediated loss of mitochondrial function and generation of reactive oxygen species during apoptosis. *J. Cell Biol.* **2003**, *160*, 65–75.

(47) Ricci, J.-E.; Munoz-Pinedo, C.; Fitzgerald, P.; Bailly-Maitre, B.; Perkins, G. A.; Yadava, N.; Scheffer, I. E.; Ellisman, M. H.; Green, D. R. Disruption of mitochondrial function during apoptosis is mediated by caspase cleavage of the p75 subunit of complex I of the electron transport chain. *Cell* **2004**, *117*, 773–786.

Caspases play an important role in apoptosis induced by immunotoxins,<sup>31</sup> although immunotoxins can kill tumor cells by a nonapoptotic pathway. Caspases also are active in apoptosis of colon cancer cells induced by NSAIDs.<sup>32</sup> When apoptosis is induced in hepatoblastoma cells by the proteasome inhibitor MG132, activation of caspase-3 occurs.<sup>37</sup> Drug-induced apoptosis in human lymphoma cells is mediated by caspase-3, which inactivates endogenous Rac GTPases.<sup>38</sup> Caspase-3 also has a role in apoptosis induced by photodynamic therapy, but not in the critical lethal event.<sup>34</sup> The activity of caspase-3 correlates strongly (negatively) with drug resistance of leukemia cells and tumors.<sup>39</sup> Other caspases, such as caspase-8 and caspase-9, appear to be more important in drug-induced apoptosis in ovarian carcinoma cells,<sup>35</sup> but not in drug-induced apoptosis in astrocytoma cells.<sup>36</sup> Other workers have evaluated the importance of caspase-8<sup>40</sup> and caspase-10<sup>41</sup> in drug-induced apoptosis; the latter is important in amplifying caspase-3 and caspase-9 activities.

When cytochrome *c* is added to cytosolic extracts from Jurkat and other cells, caspase activity starts to increase markedly after 5 min.<sup>44</sup> It is generally agreed that release of cytochrome *c* from mitochondria into the cytosol is important in the induction of apoptosis.<sup>5,45</sup> The activated caspases attack the permeabilized mitochondria, disrupting electron transport, the transmembrane potential, and structural integrity.<sup>46,47</sup> Our observations that caspase activity remains low during 2–3 h of treatment with the several drugs described here, and that mitochondrial respiration is not much affected during this time, suggest that the 2–3 h delay in the increase in caspase activity represents the time required for mitochondrial damage to occur. An increased caspase activity is observed only after mitochondrial dysfunction has become sufficient for release of cytochrome *c*. That respiration is inhibited at about the same time as caspase activity increases, for all the drugs studied, is consistent with the observation that activated caspases interfere with the action of the mitochondria.<sup>47</sup> In conclusion, caspase activation leads to impaired cellular respiration and decreased cellular ATP. Thus, the mitochondria are rapidly targeted by caspases.

## Abbreviations Used

zVAD-fmk, benzyloxycarbonyl-val-ala-asp-fluoromethylketone; Ac-DEVD-AFC, *N*-acetyl-asp-glu-val-asp-7-amino-4-trifluoromethyl coumarin; AFC, 7-amino-4-trifluoromethyl coumarin; Pt, platinum; HPLC, high-performance liquid chromatogram or chromatograph.

**Acknowledgment.** This work is supported by a fund from Paige's Butterfly Run. The technical assistance of Ms. Bonnie Toms with the cell cultures is greatly appreciated.

MP070002R